

Substantial blue carbon sequestration in the world's largest seagrass meadow

Chuancheng Fu^{1,2,3✉}, Sofia Frappi^{1,2,3}, Michelle Nicole Havlik^{1,2,3}, Wells Howe⁴, S. David Harris⁴, Elisa Laiolo^{1,2,3}, Austin J. Gallagher⁴, Pere Masqué^{5,6} & Carlos M. Duarte^{1,2,3}

Seagrass meadows are important sinks for organic carbon and provide co-benefits. However, data on the organic carbon stock in seagrass sediments are scarce for many regions, particularly The Bahamas, which accounts for up to 40.7% of the documented global seagrass area, limiting formulation of blue carbon strategies. Here, we sampled 10 seagrass meadows across an extensive island chain in The Bahamas. We estimate that Bahamas seagrass meadows store 0.42–0.59 Pg organic carbon in the top-meter sediments with an accumulation rate of 2.1–2.9 Tg annually, representing a substantial global blue carbon hotspot. Autochthonous organic carbon in sediments decreased from ~1980 onwards, with concomitant increases in cyanobacterial and mangrove contributions, suggesting disturbance of seagrass ecosystems, likely caused by tourism and maritime traffic activities. This study provides seagrass blue carbon data from a vast, understudied region and contributes to improving climate action for The Bahamas and the Greater Caribbean region.

¹Marine Science Program, Biological and Environmental Science and Engineering Division, King Abdullah University of Science and Technology (KAUST), Thuwal 23955-6900, Kingdom of Saudi Arabia. ²Red Sea Research Center (RSRC), King Abdullah University of Science and Technology, King Abdullah University of Science and Technology (KAUST), Thuwal 23955-6900, Kingdom of Saudi Arabia. ³Computational Bioscience Research Center (CBRC), King Abdullah University of Science and Technology, King Abdullah University of Science and Technology (KAUST), Thuwal 23955-6900, Kingdom of Saudi Arabia. ⁴Beneath The Waves, Herndon, VA 20172, USA. ⁵International Atomic Energy Agency (IAEA), Marine Environmental Laboratories, Quai Antoine 1er 98000, Monaco. ⁶School of Natural Sciences, Centre for Marine Ecosystems Research, Edith Cowan University, Joondalup, WA 6027, Australia. ✉email: chuancheng.fu@kaust.edu.sa

Seagrasses are angiosperms that form highly productive ecosystems in coastal areas of all continents, except for Antarctica¹. They occupy only 0.1% of the ocean surface, but can bury 27–44 Tg organic carbon (C_{org}) annually, accounting for 10–18% of the C_{org} burial in the global ocean, thus constituting an important sink in the global carbon cycle^{2,3}. Seagrass ecosystems also provide a wide range of ecosystem services, such as supporting biodiversity, fisheries, regulation of water quality, coastal protection as well as recreational and cultural values, all of which are critical for the health and well-being of humanity^{4,5}.

Recognition of the global role of seagrass as carbon sinks has led to efforts to quantify the magnitudes, sequestration rates and sources of C_{org} in seagrass sediments at different scales, required to implement “blue carbon” strategies^{3–11}. However, while these estimates placed overall boundaries on the relative C_{org} stocks and dynamics in seagrass ecosystems, considerable geographic bias exists in the available data, leading to notable information gaps, particularly for the Caribbean and Central American and African countries, which still remain poorly represented or absent in the latest global database¹¹. Obtaining regional or national estimates of C_{org} stocks and dynamics of seagrass sediments is key, as they can vary considerably between habitats, depending on multiple interrelated biogeochemical and physical factors such as seagrass traits, hydrodynamic conditions, and sediment characteristics^{3,11–13}.

The Bahamas is a large ocean nation in the subtropical Atlantic, which has been recently reported to contain the largest seagrass ecosystem in the ocean¹⁴, with an area of 66,990–92,524 km², which increased the documented global extent of seagrass by 40.7%¹⁵. Indeed, The Bahamas has a warm temperature regime, overlaid by some of the clearest waters in the ocean, and its two large carbonate sand banks act as the primary seabed substrate, favoring the extensive distribution of seagrasses¹⁴. The Bahamas has historically made very minor contributions to global greenhouse gas emissions, but it is among the world’s most vulnerable to climate change¹⁶. For example, Hurricane Dorian, in August 2019, one of the strongest Atlantic hurricanes on record and the strongest hurricane to have ever hit The Bahamas, caused about \$3.4 billion in damages, which is equal to one-quarter of The Bahamas’ annual gross domestic product (GDP)¹⁷. More importantly, as a typical small island developing state, The Bahamas rely heavily on the economic, sociocultural, and ecological integrity of their coastal areas, with the majority of their population and assets located on the coast¹⁸. For example, The Bahamas attract 7 million tourists annually, contributing to approximately 40% of its GDP¹⁹.

The discovery of the largest seagrass ecosystem in the ocean prompted the government of The Bahamas to develop new legislation enabling blue carbon strategies for climate change mitigation, adaptation and resilience²⁰. However, sediment C_{org} stocks, sequestration rates and sources of C_{org} in the Bahamian seagrass meadows remain poorly resolved and should be elucidated to support the implementation of ongoing and future blue carbon strategies. Moreover, while long-term protection offered to tiger sharks (*Galeocerdo cuvier*) in The Bahamas may have played a role in keeping seagrass habitats intact^{21,22}, tourism and urban development may lead to disturbance of these habitats. Therefore, information concerning anthropogenic pressure trajectories on seagrass ecosystem dynamics in these regions is indispensable for informing the conservation of the seagrass ecosystem and boosting action to abate pressures.

Here, we provide estimates of sediment C_{org} stock and burial rates and the dynamics in the sources of C_{org} over time in Bahamian seagrass meadows based on data from 10 seagrass meadows across an extensive island chain in The Bahamas (Fig. 1;

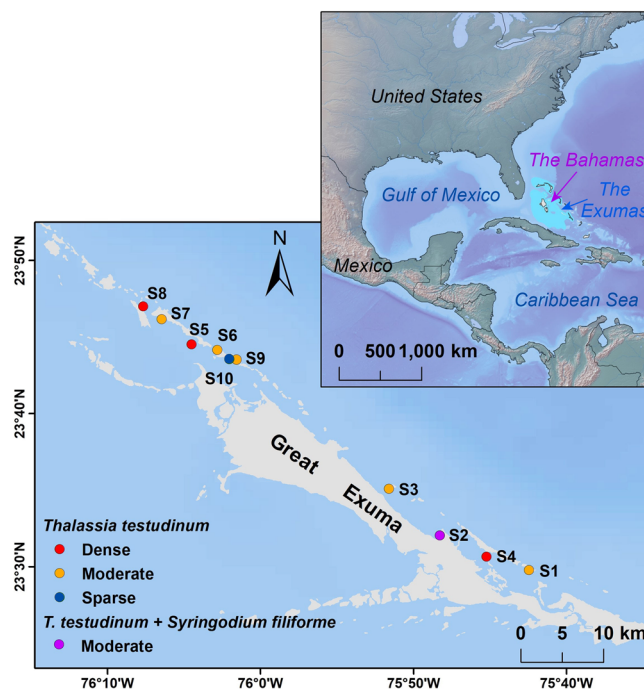


Fig. 1 Spatial distribution of seagrass sediment sampling sites in Great Exuma, a large island chain within the greater Bahamas archipelago (inset).

Map layer data sources: World shape map <https://hub.arcgis.com/>; World relief map <http://www.shadedrelief.com>; The Bahamas boundary <https://data.humdata.org/>. Sampling sites for dense, moderate, sparse *T. testudinum* meadows and mixed moderate *T. testudinum* and *S. filiforme* meadow are indicated by red, orange, blue, and purple dots, respectively.

Supplementary Table 1). The data fill a substantial geographic gap in the available information on C_{org} stocks and dynamics in the world’s largest seagrass meadow, which help improve global seagrass blue carbon estimates, thus contributing to advance seagrass-based blue carbon strategies.

Results

Magnitude of sediment organic carbon stocks. Sediment C_{org} content (% DW) along the sediment cores averaged (\pm SD) 0.74 ± 0.21 % (ranging from 0.55% to 1.03%). Dense *Thalassia testudinum* meadows showed higher C_{org} content (0.95 ± 0.21 %) in the sediments than moderate and sparse meadows (0.61 ± 0.07 % and 0.59 ± 0.04 %, respectively) ($F = 12.64$, $p = 0.005$), which showed similar values ($t = 0.08$, $p = 0.996$). Mixed *T. testudinum* and *Syringodium filiforme* meadows exhibited higher C_{org} content (0.80 ± 0.09 %) in the sediments than monospecies of *T. testudinum* ($t = 5.80$, $p = 0.013$).

Different patterns of sediment C_{org} content over depth were observed among the different meadows (Fig. 2a). In dense *T. testudinum* meadows, C_{org} contents remained relatively constant at ~ 0.9 % below 6 cm but increase to ~ 1.0 % in the upper layers ($t = -2.72$, $p = 0.025$). In comparison, sediment C_{org} contents in moderate and sparse *T. testudinum* meadows both showed minor decreasing trends from the bottom to the top of the profiles ($t = 0.75$, $p = 0.480$). The mixed *T. testudinum* and *S. filiforme* meadows, however, displayed a decrease in C_{org} contents in the top layers but a gradual increase down to the bottom of the profile ($t = 2.85$, $p = 0.012$).

Dry bulk density (DBD) along the sediment profiles averaged 0.9 ± 0.3 g cm⁻³ (ranging from 0.1 g cm⁻³ to 1.8 g cm⁻³), with no significant difference observed among the various meadows

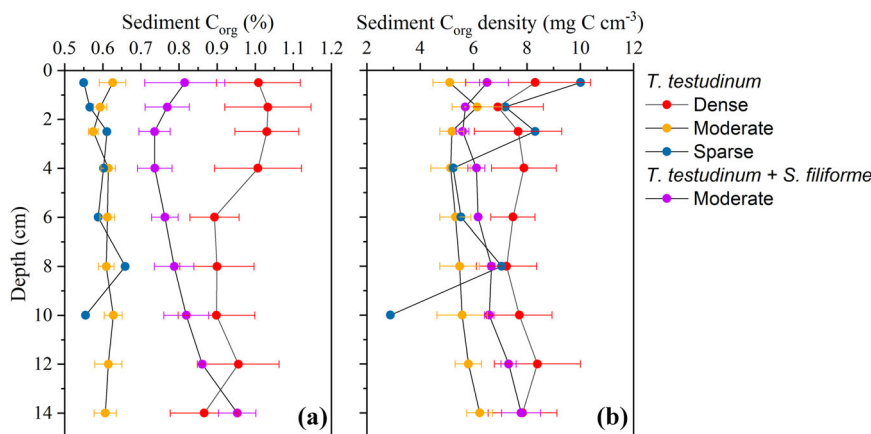


Fig. 2 Sediment organic carbon content (C_{org}) and density depth profiles of the Bahamian seagrass meadows. **a** Sediment C_{org} content depth profiles of the Bahamian seagrass meadows. **b** Sediment C_{org} density depth profiles of the Bahamian seagrass meadows. Data for dense, moderate, sparse *T. testudinum* meadows and mixed moderate *T. testudinum* and *S. filiforme* meadows are denoted by red, orange, blue, and purple dots, respectively. Data are mean values \pm standard error (SE).

Table 1 Sediment organic carbon (C_{org}) stocks in the Bahamian seagrass meadows.

Seagrass meadows	N cores	0–15 cm ($Mg C_{org} ha^{-1}$)			Extrapolated 0–100 cm ($Mg C_{org} ha^{-1}$)		
		Mean	95% CI	Range	Mean	95% CI	Range
Dense <i>T. testudinum</i>	5	11.6	3.7	6.4–17.2	77.3	25.0	42.4–114.4
Moderate <i>T. testudinum</i>	8	8.4	1.5	4.7–11.4	56.2	9.8	31.1–76.1
Sparse <i>T. testudinum</i>	1	6.7			44.6		
Moderate <i>T. testudinum</i> + <i>S. filiforme</i>	2	9.9	0.6	9.6–10.2	66.0	4.3	63.8–68.2
All	16	9.5	1.5	4.7–17.2	63.3	10.1	31.1–114.4

95% CI 95% confident interval.

($F = 2.05, p = 0.193$). DBD generally exhibited minor increasing trends from the top to the bottom of the sediment profiles ($F = 2.93, p = 0.099$), except for the sparse *T. testudinum* meadow, which displayed an anomalous significant increase in DBD towards the upper layers ($t = -4.64, p < 0.001$) (Supplementary Fig. 1).

Sediment C_{org} densities for the top 15 cm of the dense, moderate, and sparse *T. testudinum* meadows, and the mixed moderate *T. testudinum* and *S. filiforme* meadows were $7.7 \pm 3.0, 5.6 \pm 1.9, 6.6 \pm 2.3, 6.5 \pm 0.8 mg C_{org} cm^{-3}$, respectively. Sediment C_{org} density showed significant differences between dense and moderate *T. testudinum* meadows ($t = 4.82, p < 0.001$), but no significant differences were noted with other meadows. The depth pattern of sediment C_{org} density followed the same tendencies of sediment C_{org} contents in most cases (Fig. 2b). In sparse *T. testudinum* meadow, however, sediment C_{org} density increase markedly towards the surface ($t = -3.35, p = 0.001$), resulting from the anomalous increase in the DBD.

C_{org} stocks in the top 15 cm showed an increase from the sparse to the moderate and dense *T. testudinum* meadows, while no evidence for differences between monospecies of *T. testudinum* and mixed *T. testudinum* and *S. filiforme* meadows ($t = 0.24, p = 0.995$) (Table 1). Based on the newly mapped seagrass area in the Bahamas (66,990–92,524 km²)¹⁴, we estimate the seagrass sediment to contain 64–88 Tg C_{org} in the top 15 cm. The projected C_{org} stocks obtained by extrapolating to 100-cm depth would range from 44.6 (sparse *T. testudinum*) to 77.3 (dense *T. testudinum*) Mg $C_{org} ha^{-1}$, equivalent to a total inventory of 424–586 Tg C_{org} in the top-meter sediment of the Bahamas seagrass ecosystem.

Organic carbon accumulation rates. Four of the nine sediment cores analyzed (S3, S7, S9 and S10) conformed to a ²¹⁰Pb pattern of decreasing concentrations from the surface towards deeper layers, while the rest of them showed anomalies suggesting the presence of some degree of mixing (Supplementary Fig. 2). Sediment mixing may lead to the overestimation of sediment accumulation rates (SARs)²³, hence where mixing is present (i.e., in cores S2, S3, S7, S8), rates should be considered as upper limits. Core S1 showed no decreasing trend of the ²¹⁰Pb concentrations with depth, reflecting intense mixing and rendered it undatable.

The SARs of dense, moderate, sparse *T. testudinum* and mixed moderate *T. testudinum* and *S. filiforme* meadows over the last century are (\pm SE) $1.9 \pm 0.2, 4.5 \pm 1.3, 4.0 \pm 0.5$ and $1.0 \pm 0.1 mm yr^{-1}$, respectively. The corresponding C_{org} accumulation rates (CAR) over the last century are $28 \pm 5, 37 \pm 15, 38 \pm 5$ and $4 \pm 1 g C_{org} m^{-2} yr^{-1}$, respectively (Table 2). Extrapolating to the total seagrass area, we estimate the Bahamian seagrass sediment annually sequester 2.1–2.9 Tg C_{org} .

Organic carbon sources. Seagrass sediments had an average stable C_{org} isotope ($\delta^{13}C$) value (\pm SD) and carbon-nitrogen molar ratio (C/N) of $-13.9 \pm 1.6 ‰$ and 11.1 ± 2.8 throughout the sampled meadows and thickness of the deposits, respectively (Fig. 3). $\delta^{13}C$ values were similar between the moderate and sparse *T. testudinum* meadows ($-14.9 \pm 1.4 ‰$ and $-14.7 \pm 0.6 ‰$, respectively; $t = -0.15, p = 0.988$), while both were significantly lighter than the dense meadows ($-12.5 \pm 0.9 ‰$) ($F = 3.94, p = 0.004$). The mixed *T. testudinum* and *S. filiforme* meadows showed significantly heavier $\delta^{13}C$ values ($-12.8 \pm 0.6 ‰$) than the monospecies of *T. testudinum* ($t = -6.50, p < 0.001$), whereas

Table 2 Sediment and organic carbon accumulation rates in the Bahamian seagrass meadows.

Seagrass species	N cores	SAR (mm yr ⁻¹)		MAR (g cm ⁻² yr ⁻¹)		CAR (g C _{org} m ⁻² yr ⁻¹)	
		Mean	SE	Mean	SE	Mean	SE
Dense <i>T. testudinum</i>	2	1.9	0.2	0.27	0.01	28	5
Moderate <i>T. testudinum</i>	4	4.5	1.3	0.61	0.24	37	15
Sparse <i>T. testudinum</i>	1	4.0	0.5	0.65	0.08	38	5
Moderate <i>T. testudinum</i> + <i>S. filiforme</i>	1	1.0	0.1	0.05	0.01	4	1
All	8	3.3	0.8	0.46	0.14	31	8

SAR sediment accumulation rate, MAR mass accumulation rate, CAR organic carbon accumulation rate, SE standard error.

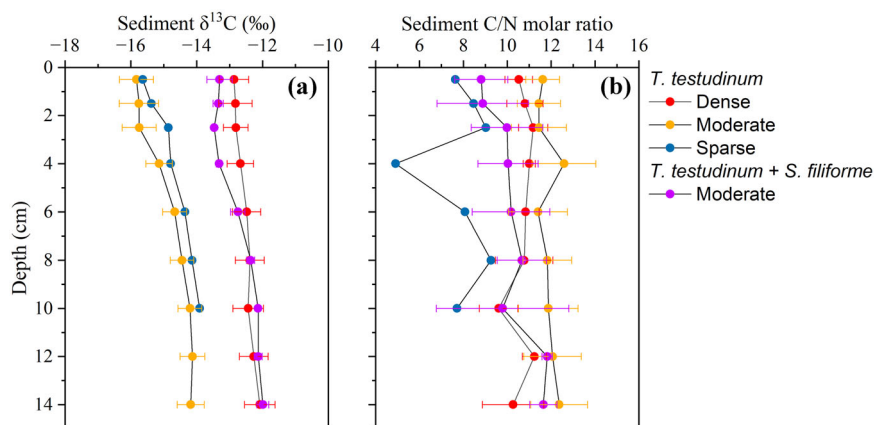


Fig. 3 Sediment $\delta^{13}\text{C}$ and C/N molar ratio depth profiles of the Bahamian seagrass meadows. **a** Sediment $\delta^{13}\text{C}$ depth profiles of the Bahamian seagrass meadows. **b** Sediment C/N molar depth profiles of the Bahamian seagrass meadows. Data for dense, moderate, sparse *T. testudinum* meadows and mixed moderate *T. testudinum* and *S. filiforme* meadows are denoted by red, orange, blue, and purple dots, respectively. Data are mean values \pm SE.

C/N ratios showed an opposite trend ($t = 2.03$, $p = 0.045$). *T. testudinum* seagrass C/N ratios follow the sequence of moderate > dense > sparse meadows (11.8 ± 3.3 , 10.7 ± 1.8 , and 7.9 ± 1.4 , respectively). However, sediment C/N lacks a strong pattern across sediment depth ($F = 1.51$, $p = 0.221$), in contrast to $\delta^{13}\text{C}$, which progressively decreases (i.e., more depleted) towards the top ($F = 38.23$, $P < 0.001$). By applying a Bayesian mixing model with $\delta^{13}\text{C}$ and C/N tracers, we estimated that seagrass detritus contributed $29 \pm 18\%$, $24 \pm 15\%$, $24 \pm 15\%$ and $30 \pm 19\%$ to the sediments C_{org} pool in dense, moderate, sparse *T. testudinum* and moderate mixed *T. testudinum* and *S. filiforme* meadows, respectively. Allochthonous contribution was dominated by cyanobacteria (28–35%), followed by algae and phytoplankton (27–28%), and was lower for mangroves (14–15%).

The age model of each seagrass sediment cores allowed us to explore the C_{org} source changes over time (Fig. 4). The dated layers of the sediment cores spanned 11–76 years as a result of different SARs. The autochthonous and allochthonous sources display two distinct patterns across the sediment cores, respectively. Moderate (S3 and S6) and sparse (S10) *T. testudinum* seagrass meadows showed steep decreases in seagrass-derived C_{org} from ~1980 onwards, accompanied by increased contributions of cyanobacteria and mangrove-derived C_{org}. However, these trends were less pronounced in the remaining meadows, especially the dense *T. testudinum* seagrass meadow (S5), which exhibited minor decreases in seagrass-derived C_{org} and slight increases in cyanobacteria and mangrove-derived C_{org} at the same period. Algal and phytoplankton C_{org} inputs to the sediment were relative stable, but began to decrease after ~2000s for S3, S6, and S10.

Discussion

Bahamian seagrass meadow as a global hotspot of blue carbon sequestration. Sediment C_{org} stock per unit area of the Bahamian seagrass meadows is slightly lower than reported global averages (top 15 cm, $11.6 \text{ Mg C}_{\text{org}} \text{ ha}^{-1}$; top 1 m, $77.0 \text{ Mg C}_{\text{org}} \text{ ha}^{-1}$)¹¹, but the CAR are well below the global mean estimates ($139 \text{ g C}_{\text{org}} \text{ m}^{-2} \text{ yr}^{-1}$)⁴. When compared to literature estimates of C_{org} storage and CAR in carbonate seagrass meadows at similar latitudes globally (Supplementary Table 2), C_{org} storage and accumulation in The Bahamas are generally in the lower range on a spatial basis. The C_{org} stocks align with those of the seagrass meadows in Southeastern Brazil ($67.6 \pm 14.7 \text{ Mg C}_{\text{org}} \text{ ha}^{-1}$), despite higher biomass of the seagrass species in The Bahamas^{24,25}. Meanwhile, our C_{org} stock estimates fall within the range of those reported for arid regions with extreme environmental conditions (i.e., nutrient limitation and high temperature), such as seagrass meadows around the carbonate-rich sediments of the Arabian Peninsula, documented to have low C_{org} sink capacity ($34.3\text{--}76.2 \text{ Mg C}_{\text{org}} \text{ ha}^{-1}$)^{8,26,27}. Although CAR in Bahamian seagrass meadows is 2–3 fold higher than those in the arid regions, it only represents 1/6 and 1/2 of those in Florida Bay and Shark Bay, respectively^{25,28,29}. These comparisons suggest that The Bahamas seagrass ecosystem is not as efficient in accumulating C_{org} in the underlying sediments per unit area, as those elsewhere.

The relatively low C_{org} stocks and accumulation rates in Bahamian seagrass meadows are consistent with the low reported net primary production (NPP) of seagrasses in this region, which is only half of the global values (The Bahamas: $213.1 \text{ g C}_{\text{org}} \text{ m}^{-2} \text{ yr}^{-1}$;³⁰ Global: $394\text{--}449 \text{ g C}_{\text{org}} \text{ m}^{-2} \text{ yr}^{-1}$)³¹, as well as a comparatively low biomass^{24,32,33}. It is, therefore, reasonable to

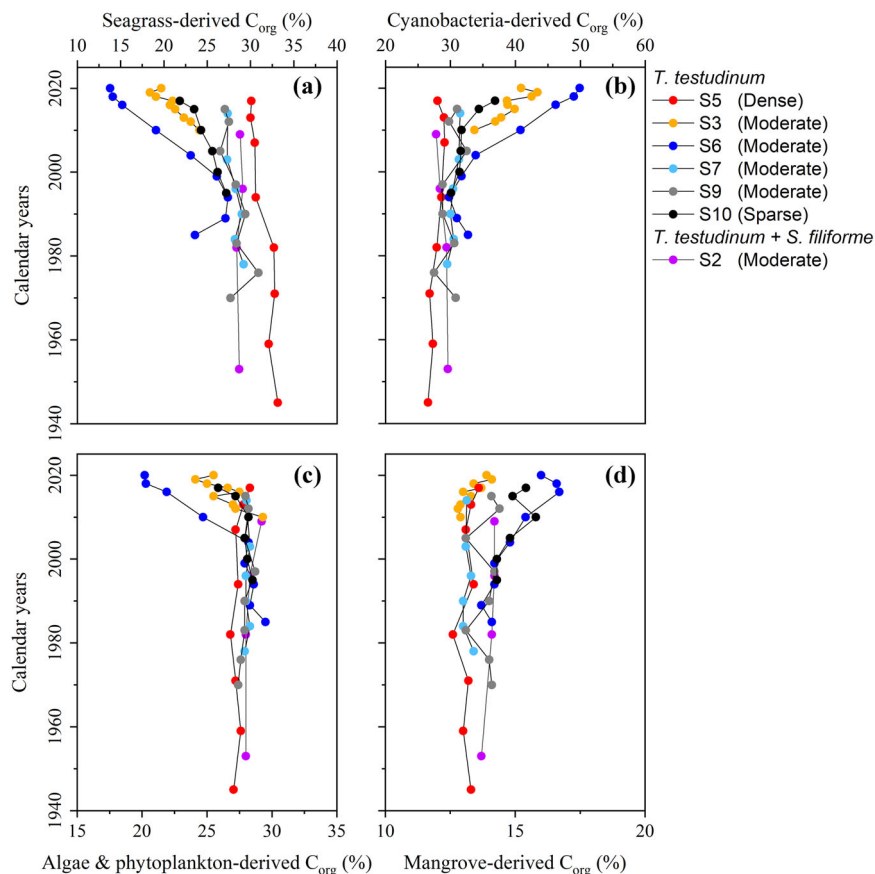


Fig. 4 Temporal trends of sediment organic carbon (C_{org}) sources in the Bahamian seagrass meadows. **a** Temporal trends of seagrass-derived C_{org} in the Bahamian seagrass meadows. **b** Temporal trends of cyanobacteria-derived C_{org} in the Bahamian seagrass meadows. **c** Temporal trends of Algae & phytoplankton-derived C_{org} in the Bahamian seagrass meadows. **d** Temporal trends of mangrove-derived C_{org} in the Bahamian seagrass meadows. Data for core S5 (dense *T. testudinum*), S3 (moderate *T. testudinum*), S6 (moderate *T. testudinum*), S7 (moderate *T. testudinum*), S9 (moderate *T. testudinum*), S10 (sparse *T. testudinum*), and S2 (mixed moderate *T. testudinum* and *S. filiforme*) are denoted by red, orange, blue, light blue, gray, black, and purple dots, respectively.

expect low C_{org} stocks in the underlying sediment, since seagrass plant traits (e.g., density) are one of the key drivers of seagrass sediment C_{org} stocks^{11,13}, also evidenced by the differences detected among seagrass habitats with different plant densities in our results. The low NPP of the Bahamian seagrass could probably be due to phosphorous limitation, as a result of the remote nature of The Bahama Banks leading to limited terrestrial sediment supply, as well as binding of inorganic phosphate by biogenic carbonate sediment^{34,35}. Yet, the buried C_{org} in sediment, representing 11% of NPP in the Bahamian seagrass meadows, is somewhat below the estimated global ratio (16%)³¹. Several complementary reasons can explain this. The SARs of the studied seagrass meadows are relatively low and mainly determined by the production and redistribution of chemical and biogenic carbonates^{36–38}, with frequent presence of mixing of the sediment due to physical disturbance or bioturbations that may promote more decomposition of deposited C_{org} . In fact, the carbonates in the sampled region are relatively coarse in grain size and contain a large proportion of oolitic particles³⁹. C_{org} in coarse carbonate sedimentary matrix may cycle rapidly, and even encapsulation into crystals does not fully protect it from decomposition or alteration⁴⁰. Finally, dissolution rates of carbonates in seagrasses can be an important loss driver for carbonate in The Bahamas⁴¹, reducing the sediment buildup and releasing C_{org} contained in the carbonate matrix, rendering C_{org} vulnerable to decomposition.

Yet, The Bahamas Banks host the world's largest seagrass ecosystems, which accounts for 25.1–40.7 % of the documented global seagrass extent (227,377–266,562 km²)^{14,15}. The C_{org} values obtained here (0.4–1.4 %) are consistent with ancillary values previously reported for The Bahamas (<0.5–1.8 %)^{33,42,43}. This supports the extrapolation from our values to The Bahamas seagrass ecosystem, which delivers a mean C_{org} stock corresponding to 20.5–33.7 % of the global seagrass C_{org} stock (1.75–2.05 Pg C_{org})^{11,15}, and 5.7–9.2 % of total annual seagrass sediment C_{org} sequestration (31.4–36.8 Tg C_{org} yr⁻¹)^{4,15}, based on documented global seagrass extent (Table 3). Taken together, these findings suggest that the Bahamas seagrass meadows render the overall ecosystem a global blue carbon hotspot.

Extensive seagrass ecosystems over the Bahamas Banks provide critical opportunities to mitigate climate change. Indeed, we estimate that its annual C_{org} sequestration is equivalent to or even higher than the anthropogenic greenhouse gas emissions in the Bahamas (1.71 Tg C yr⁻¹ at 2018 rates)⁴⁴. Moreover, The Bahamas Banks are generally less than 10 m deep and are bounded by near-vertical declivities into very deep water, which likely facilitate the export of seagrass carbon to the deep ocean^{45,46}. Following the estimation by Duarte and Krause-Jensen⁴⁵ that 4.9% of the seagrass NPP could be sequestered in the deep ocean, we estimate that The Bahamas seagrass meadows can contribute roughly 10.4 g C_{org} m⁻² yr⁻¹ and a total of 0.70–0.96 Tg C_{org} to C_{org} sequestration in the deep-sea annually.

Table 3 Extent, organic carbon accumulation rates and stocks (in the top meter of sediment) in the global and Bahamian seagrass meadows.

Seagrass ecosystem	Seagrass Area (km ²)		Sediment CAR (Tg C _{org} yr ⁻¹)		Sediment C _{org} stock (Pg)	
	Min.	Max.	Min.	Max.	Min.	Max.
Global (documented)	227,377 ^{14,15}	266,562 ¹⁵	31.4 ^{4,14,15}	36.8 ^{4,15}	1.75 ^{11,14,15}	2.05 ^{11,15}
Bahamian	66,990 ¹⁴	92,524 ¹⁴	2.1	2.9	0.42	0.59
Bahamian/Global	25.1%	40.7%	5.7%	9.2%	20.5%	33.7%

CAR organic carbon accumulation rate, C_{org} organic carbon, Min. minimum, Max. maximum.

In addition, our estimates of sediment accumulation rates show that The Bahamas seagrass meadows elevate the seabed at a mean rate of $3.3 \pm 1.5 \text{ mm yr}^{-1}$, well exceeding the rate of sea level rise in The Bahamas (0.2 mm yr^{-1})⁴⁷. Given that the Bahamas is an archipelago with the majority of its population and assets located near the coast for geographical and economic reasons, the natural shoreline protection provided by seagrass meadows from sea level rise is particularly important to the climate-change mitigation of this nation.

Seagrass disturbance revealed by sediment C_{org} source change.

Seagrass sediment carbon source apportionment shows that the autochthonous C_{org} in The Bahamas sediments is lower than estimates for seagrasses globally (~50%)⁴⁸. This difference is probably due to the relatively low NPP of Bahamian seagrass meadows. Grazing may also be an important factor, through herbivores such as green turtles and conch^{43,49}. Although long-term protection offered to tiger sharks in The Bahamas has likely helped to keep seagrass habitats from overgrazing through the top-down control of grazers¹⁴, our findings revealed a simultaneous decline of seagrass-derived C_{org} in sediments after the 1980s, indicating disturbance of seagrasses around The Exumas. However, the declines in seagrass-derived C_{org} are not uniform across the sites, which is likely related to the intensity, duration and frequency of exposure to disturbances⁵⁰. Overall, the contribution of seagrass to C_{org} stocks declined from $(29 \pm 3) \%$ in the 1980's to $(21 \pm 7) \%$ in the 2020's, suggesting a parallel decline in seagrass NPP in the region, likely resulting from anthropogenic impacts. Indeed, the Bahamas' GDP has grown at least 10-fold from the 1980s to the present, with tourism revenues dominating (~40%)¹⁹. Before the impact of COVID (2019), tourist numbers had at least doubled to over 7 million, which was about 18-times the population of The Bahamas¹⁹. Meanwhile, The Bahamas has become a major hub for international marine traffic, with more than 5,000 vessels, including a number of mega-yachts, transiting the Bahamas Banks every year. The intensified boating, anchoring, yachts, shipping activities, and dredging for coastal infrastructure associated with tourism and marine traffic development^{32,50,51} may have contributed to seagrass disturbance in the study area, therefore leading to decline in seagrass C_{org} input to the sediments. Moreover, these declines were in parallel with decreases in algae and phytoplankton-derived C_{org} after ~2000s, possibly attributed to the decline in epiphytes resulting from seagrass disturbance⁵².

Cyanobacteria contribute much more to sediment C_{org} than seagrasses, which is counterintuitive given their low biomass and limited nutrient availability in the study area. This could be explained by the intercrystalline and intracrystalline protection of cyanobacteria-derived C_{org} as they are involved in the development of ooids⁵³. In contrast to autochthonous input, cyanobacteria-derived C_{org} in seagrass sediment increased at different degrees since the 1980s and appeared to be widespread.

Anchoring, fishing, as well as dredging activities in all lead to disturbance and suspension of bottom sediments^{32,50,51}, which might release nutrients such as phosphorus and iron into the water column. This will alleviate nutrient limitation and stimulate cyanobacteria blooms in the water column and lead to increased cyanobacterial contributions to sediment C_{org} over time. In addition, Sahara dust is suggested as a major source of nutrients to the Caribbean supporting cyanobacteria in the Bahamas seascape⁵⁴. Increased dust deposition and precipitation over the past few decades⁵⁵ concurrent with seagrass decline may also partially explain the increase in cyanobacteria-derived C_{org} in seagrass sediment.

Furthermore, presence of C_{org} derived from adjacent mangrove habitats to the seagrass sediments emphasizes the importance of cross-habitat connectivity within the tropical coastal seascape. Mangrove-derived C_{org} in sediments was relatively stable before 1980s but increased slightly since then, which might be associated with the onset of mangrove disturbance due to anthropogenic and natural drivers. Indeed, deforestation, tidal flow change due to silt blocking the entrances to creeks, harvest for charcoal production, as well as increased tropical storms and hurricanes have resulted in 22% of mangrove loss in the Bahamas from 1980 to 2005⁵⁶. More strikingly, catastrophic hurricanes, such as Dorian in 2019, destroyed 30% (~7,776 ha) of mangroves around the islands of Grand Bahama and Abaco⁵⁷. These disturbances may possibly result in an escalated export of C_{org} from deforested mangrove soils⁵⁸, which explains the increase of mangrove-derived C_{org} in seagrass sediment after 1970s.

Conclusions

Our data suggest The Bahamas seagrass ecosystem is a substantial global blue carbon hotspot, its meadows containing stocks of C_{org} (0.42–0.59 Pg) equivalent to 20.5–33.7 % of global seagrass sediment estimates and 5.7–9.2 % of annual worldwide sequestration rates, estimated based on documented global extent. Our data add to the growing body of knowledge on C_{org} storage and sequestration in seagrass meadows and provide values for a relatively data-deficient region that supports the largest seagrass ecosystem in the ocean. Further efforts are, however, required to map C_{org} stocks and sequestration more expansively across this vast region, as well as consolidating potential additional contributions to carbon dioxide sequestration from alkalinity release in seagrass meadows. In addition, an understanding of the carbon budget of seagrass meadows compared to bare areas is essential to consolidate the role of seagrass in carbon dioxide removal. Our results provide evidence for declines of carbon burial in Bahamian seagrass meadows since the 1980's, suggesting opportunities to enhance carbon sequestration through blue carbon strategies aimed at avoiding further losses and restoring Bahamas seagrass meadows, as well as damaged mangrove forests. Moreover, the conserved and restored seagrass meadows will provide essential co-benefits to The Bahamas such as coastal protection from sea

level rise and increased hurricanes, thereby adding resilience to future climate change.

Methods

Sediment sampling. This study was conducted in The Exuma Cays, an extensive set of 365 low-lying islands spanning 209 km north-south, centrally located on the Great Bahamas Bank within the broader Bahamas archipelago. The shallow waters of The Exumas support extensive monospecific *T. testudinum* meadows and mixed *T. testudinum* and *S. filiforme* meadows. The Exumas are a world-famous tourist and yachting destination, with a wide range of exclusive resorts, hotels and marinas which constitute the primary economic income, along with fisheries.

In total, sediment coring was performed in 10 sites containing seagrass meadows between 17th and 23rd November 2021, distributed along the Great Exuma island chain (Fig. 1), mostly consisting of *T. testudinum* meadows of variable density and one mixed *T. testudinum* and *S. filiforme* meadow (Supplementary Table 1). Seagrass meadow coverage was estimated through two complementary methods. Initially, the seagrass coverage was categorized into three types: dense (coverage > 70%), moderate (coverage 30–70%), and sparse (coverage < 30%), in accordance with the classification by Wabnitz et al.⁵⁹. An initial evaluation of seagrass coverage within these categories was performed through visual estimation during sediment sample collection. Vegetation species at each sampling site were identified based on expert knowledge. Secondly, during field expeditions, photographs of the seagrass meadows were captured. An image thresholding technique available in ImageJ (v. 1.53e) was employed⁶⁰, to assess seagrass cover percentage in each photo¹⁴. The seagrass meadows were subsequently categorized into dense, moderate, and sparse seagrass coverage as remarked. These estimations can then validate visual estimation during sediment sample collection (Supplementary Table 3).

Two to three sediment cores were extracted at each meadow sites, resulting in a total of 25 cores for C_{org} and ^{210}Pb analyses. All cores were collected by SCUBA divers, by inserting PVC pipes of 30 cm long, 9.4 cm in diameter and >60 cm long, 7 cm in diameter, respectively. From each site, one or two 15 cm long sediment cores (except for S10, which was sampled up to a depth of 11 cm) were used for C_{org} stock and source analyses (referred as C_{org} core), and one sediment core between 24 and 56 cm long was used for ^{210}Pb measurements (referred as ^{210}Pb core). One of the stations (S4, Fig. 1), was discarded for sediment chronology due to evident bioturbation due to thalassinidea shrimp. Compression of the sediments during coring was alleviated by distributing the spatial discordances proportionally between the expected and the observed sediment column layers²⁹. The compression of the ^{210}Pb core during coring ranged from 5% to 22%, and no compression was observed for the shorter C_{org} cores. The C_{org} cores were sliced at 1 cm thick interval for the top 3 cm and at 2 cm thick interval down to the bottom. The ^{210}Pb corers were cut into 0.5 cm thick slices for the top 1–3 cm and 1 cm thick slices down to the bottom of the core.

Sediment dry bulk density, organic carbon, nitrogen and organic carbon isotope analysis. Each sediment slice was weighed before and after oven drying at 60 °C until constant weight to determine the dry bulk density (DBD) by dividing the dry weight by the sample fresh volume (cm³)⁶¹. All visible plant, faunal, and large inorganic material (e.g., shells) were removed, and the sediment was crushed using an agate mortar and pestle to obtain a homogenized fine sample.

An aliquot of the grinded sediment sample was weighed accurately into silver capsules and acidified with 4% HCl to

remove carbonates until no effervescence was detected in two consecutive cycles. The samples were dried in a 60 °C oven overnight, and then encapsulated into tin capsules. One subsample was left untreated in order to measure total nitrogen (TN). All the samples from C_{org} cores were analyzed for C_{org} and TN using an Organic Elemental Analyzer Flash 2000 (Thermo Fisher Scientific, Waltham, MA). For sediment $\delta^{13}C$ quantification, about 2 g subsamples were acidified with 1 mol L⁻¹ HCl to remove carbonates, centrifuged, and the supernatant was carefully removed by pipette, avoiding resuspension. The sample was then rinsed with Milli-Q water twice, centrifuged and the supernatant removed. The residual samples were re-dried in a 60 °C oven and then loaded onto tin capsules for $\delta^{13}C$ analyses by using a cavity ring-down spectrometer system by Picarro (CM-CRDS G2201-I, Picarro, Santa Clara, CA) attached to a combustion module (Costech Analytical Technologies, Valencia, CA). Replicate samples accounted for 10% with measurement errors of $\pm 0.04\%$, $\pm 0.003\%$ and $\pm 0.2\%$ for C_{org} , TN and $\delta^{13}C$, respectively. Sediment C_{org} stocks (Mg C_{org} ha⁻¹) within each core were then estimated by calculating the cumulative C_{org} stock (multiplying C_{org} density by the depth interval) downcore.

Sediment ^{210}Pb analysis. The concentrations of ^{210}Pb along the nine ^{210}Pb cores were analyzed aiming to determine sediment accumulation rates during the past century/decades, where feasible. ^{210}Pb was determined through the quantification of its decay product ^{210}Po activity (assuming radioactive equilibrium between the two radionuclides) by alpha spectrometry after addition of ^{209}Po as an internal tracer, digestion in a HNO₃:HF mixture (9: 3 mL) using an analytical microwave oven and plating onto silver disks⁶². ^{226}Ra (supported ^{210}Pb) was analyzed in two to four selected slices from the upper and lower sections of each core by gamma spectrometry through the emission lines of its decay product ^{214}Pb . Analyses of replicate samples and reference materials were carried out systematically to ensure the accuracy and the precision of the results. The concentrations of excess ^{210}Pb used to apply the age models were determined as the difference between total ^{210}Pb and ^{226}Ra . The mean mass and sediment accumulation rates (MAR and SAR, respectively) over the past decades/century could be calculated for eight of the nine dated sediment cores using the Constant Flux-Constant Sedimentation (CF-CS) model below the surface mixed layers^{23,63} (Supplementary Fig. 2). Carbon accumulation rates (CAR) were estimated as the product of the fraction of % C_{org} and the MAR. We adopt the mean MAR values to reconstruct the age models of the C_{org} cores based on the mass depth of each core, which therefore allow us to investigate the C_{org} source change over time. However, it was not possible to establish an age model for S8 due to sediment mixing throughout the top 15 cm of the C_{org} core.

Sediment C_{org} source estimation. A Bayesian mixing model (package *simmr*⁶⁴) in R 4.3.0⁶⁵ was used to estimate the relative contribution of the potential C_{org} sources to the sediment C_{org} stock. Two tracers ($\delta^{13}C$ and C/N molar ratio) were used and four endmembers were considered as potential sources in the mixing model, namely seagrass, cyanobacteria, algae (macroalgae and epiphyte) and phytoplankton, and mangrove. Cyanobacteria was included because of empirical evidence that cyanobacteria involvement in the development of ooids from The Bahama Banks, and is preserved as intercrystalline and intracrystalline carbon⁵³.

A total of 15 large seagrass fragment (leaves and rhizomes) samples were collected from the C_{org} cores and analyzed for $\delta^{13}C$ values, C_{org} and TN concentrations. We did so to account for the significant decomposition effects on $\delta^{13}C$ signature and C/N

ratio^{66,67}. The fragment samples were washed with Milli-Q water, fumed with HCl to remove carbonates and then dried at 60 °C⁶⁸. Fragment $\delta^{13}\text{C}$, C_{org} and TN were analyzed using the same instruments for sediment samples. We also synthesized $\delta^{13}\text{C}$ and C/N ratio data for cyanobacteria, macroalgae, epiphyte, phytoplankton and mangrove plants from The Bahamas to generate corresponding endmembers. The available data for the $\delta^{13}\text{C}$ and C/N ratio of seagrass epiphytes and phytoplankton often indicate that these fall within the same range as macroalgal $\delta^{13}\text{C}$ and C/N ratio (Supplementary Table 4). Therefore, we pooled seagrass epiphytes and phytoplankton collectively with macroalgae as a single C_{org} source (Supplementary Table 4). We did not consider terrestrial C_{org} input as suggested for other estuarine regimes, because of the minimal land area of The Bahamas, where rivers are absent. Due to the large variation in $\delta^{13}\text{C}$ and C/N among these endmembers, we used the median values of isotope or C/N ratio since it was difficult to deduce undisputed fractionation factors for them⁶⁹.

Statistical analysis. We used linear mixed-effect models (“lme()” function in R 4.3.0^{65,70}) with restricted maximum likelihood (REML) estimates to assess potential variability in sediment parameters (C_{org} , DBD, C_{org} density, $\delta^{13}\text{C}$ and C/N molar ratio) among different seagrass meadows. Sampling location was included as a random factor and Tukey posthoc tests were employed to assess pairwise differences among species and sediment depths. Variability of C_{org} stock in the top 15 cm of sediment among different seagrass species was not tested due to sample number limitation. The projected C_{org} stock in the upper meter of sediment was estimated by multiplying the C_{org} stock by 100/15 to extrapolate the C_{org} stocks to 100-cm depth and given as extrapolated C_{org} stock, to enable comparison with literature values³. We did not consider variance of C_{org} stock over depth due to divergent patterns of C_{org} among different seagrass meadows observed in this study. However, a major limitation of this approach is that the transformation could lead to an uncertainty of C_{org} stocks since the top core section contains typically more C_{org} than the older bottom section³. Data plotting was conducted using OriginPro 2023 (OriginLab, Northampton, MA)

Reporting summary. Further information on research design is available in the Nature Portfolio Reporting Summary linked to this article.

Data availability

The data that support the findings of this study are available at Figshare database (<https://doi.org/10.6084/m9.figshare.24418201>).

Received: 7 June 2023; Accepted: 1 December 2023;

Published online: 13 December 2023

References

- Hemminga, M. A., & Duarte, C. M. *Seagrass Ecology* (Cambridge University Press, 2000).
- Duarte, C. M., Middelburg, J. J. & Caraco, N. Major role of marine vegetation on the oceanic carbon cycle. *Biogeosciences* **2**, 1–8 (2005).
- Fourqurean, J. W. et al. Seagrass ecosystems as a globally significant carbon stock. *Nat. Geosci.* **5**, 505–509 (2012).
- Duarte, C. M., Losada, I. J., Hendriks, I. E., Mazarrasa, I. & Marbà, N. The role of coastal plant communities for climate change mitigation and adaptation. *Nat. Clim. Change* **3**, 961–968 (2013).
- Unsworth, R. K., Cullen-Unsworth, L. C., Jones, B. L. & Lilley, R. J. The planetary role of seagrass conservation. *Science* **377**, 609–613 (2022).
- Nellemann, C. et al (eds). *Blue Carbon: the Role of Healthy Oceans in Binding Carbon: A Rapid Response Assessment* (United Nations Environment Programme, 2009).
- McLeod, E. et al. A blueprint for blue carbon: toward an improved understanding of the role of vegetated coastal habitats in sequestering CO₂. *Front. Ecol. Environ.* **9**, 552–CO560 (2011).
- Campbell, J. E., Lacey, E. A., Decker, R. A., Crooks, S. & Fourqurean, J. W. Carbon storage in seagrass beds of Abu Dhabi, United Arab Emirates. *Estuar. Coast.* **38**, 242–251 (2015).
- Serrano, O. et al. Australian vegetated coastal ecosystems as global hotspots for climate change mitigation. *Nat. Commun.* **10**, 4313 (2019).
- Macreadie, P. I. et al. Blue carbon as a natural climate solution. *Nat. Rev. Earth Environ.* **2**, 826–839 (2021).
- Kennedy, H. et al. Species traits and geomorphic setting as drivers of global soil carbon stocks in seagrass meadows. *Global Biogeochem. Cycles* **36**, e2022GB007481 (2022).
- Gullström, M. et al. Blue carbon storage in tropical seagrass meadows relates to carbonate stock dynamics, plant–sediment processes, and landscape context: insights from the western Indian Ocean. *Ecosystems* **21**, 551–566 (2018).
- Mazarrasa, I. et al. Factors determining seagrass Blue Carbon across bioregions and geomorphologies. *Global Biogeochem. Cycles* **35**, e2021GB006935 (2021).
- Gallagher, A. J. et al. Tiger sharks support the characterization of the world’s largest seagrass ecosystem. *Nat. Commun.* **13**, 6328 (2022).
- McKenzie, L. J. et al. The global distribution of seagrass meadows. *Environ. Res. Lett.* **15**, 074041 (2020).
- Pan American Health Organization. Caribbean Action Plan on Health and Climate Change. Washington, D.C. https://iris.paho.org/bitstream/handle/10665.2/38566/PAHOCDE19007_eng.pdf (2020).
- Reliefweb. *The facts: Hurricane Dorian’s devastating effect on The Bahamas.* <https://reliefweb.int/report/bahamas/facts-hurricane-dorian-s-devastating-effect-bahamas> (2020).
- Sealy, K. S. & Strobl, E. A hurricane loss risk assessment of coastal properties in the Caribbean: Evidence from the Bahamas. *Ocean Coast. Manag.* **149**, 42–51 (2017).
- The Bahamas National Statistical Institute, & Ministry of Economic Affairs. *National Accounts Annual Report 2021.* <https://www.bahamas.gov.bs/wps/wcm/connect/6e3cf7da-b3f4-46f9-8c09-4157fb451ba0/National+Accounts+Annual+Report+2021.pdf?MOD=AJPERES> (2021).
- The Bahamas. Climate Change and Carbon Market Initiatives Act. [https://www.fao.org/faolex/results/details/en/c/LEX-FAOC211771\(No..initiatives%20to%20offset%20carbon%20emissions/#:~:text=Bahamas-Climate%20Change%20and%20Carbon%20Market%20Initiatives%20Act%2C%202022%20\(2022\)\)](https://www.fao.org/faolex/results/details/en/c/LEX-FAOC211771(No..initiatives%20to%20offset%20carbon%20emissions/#:~:text=Bahamas-Climate%20Change%20and%20Carbon%20Market%20Initiatives%20Act%2C%202022%20(2022)))
- Gallagher, A. J. et al. Spatial connectivity and drivers of shark habitat use within a large marine protected area in the Caribbean. *The Bahamas Shark Sanctuary. Front. Mar. Sci.* **7**, 1223 (2021).
- Gallagher, A. J. et al. The Caribbean needs big marine protected areas. *Science* **367**, 749–749 (2020).
- Arias-Ortiz, A. et al. Reviews and syntheses: ²¹⁰Pb-derived sediment and carbon accumulation rates in vegetated coastal ecosystems—setting the record straight. *Biogeosciences* **15**, 6791–6818 (2018).
- Duarte, C. M. & Chiscano, C. L. Seagrass biomass and production: a reassessment. *Aquat. Bot.* **65**, 159–174 (1999).
- Howard, J. L., Creed, J. C., Aguiar, M. V. & Fourqurean, J. W. CO₂ released by carbonate sediment production in some coastal areas may offset the benefits of seagrass “Blue Carbon” storage. *Limnol. Oceanogr.* **63**, 160–172 (2018).
- Cusack, M. et al. Organic carbon sequestration and storage in vegetated coastal habitats along the western coast of the Arabian Gulf. *Environ. Res. Lett.* **13**, 074007 (2018).
- Serrano, O., Almahasheer, H., Duarte, C. M. & Irigoien, X. Carbon stocks and accumulation rates in Red Sea seagrass meadows. *Sci. Rep.* **8**, 1–13 (2018).
- Cheng, J., Collins, L. S. & Holmes, C. Four thousand years of habitat change in Florida Bay as indicated by benthic foraminifera. *J. Foraminiferal Res.* **42**, 3–17 (2012).
- Arias-Ortiz, A. et al. A marine heatwave drives massive losses from the world’s largest seagrass carbon stocks. *Nat. Clim. Change* **8**, 338–344 (2018).
- Dierssen, H. M., Zimmerman, R. C., Drake, L. A. & Burdige, D. Benthic ecology from space: optics and net primary production in seagrass and benthic algae across the Great Bahama Bank. *Mar. Ecol. Prog. Ser.* **411**, 1–15 (2010).
- Duarte, C. M. Reviews and syntheses: Hidden forests, the role of vegetated coastal habitats in the ocean carbon budget. *Biogeosciences* **14**, 301–310 (2017).
- Buchan, K. C. The Bahamas. *Mar. Pollut. Bull.* **41**, 94–111 (2000).
- Burdige, D. J. & Zimmerman, R. C. Impact of sea grass density on carbonate dissolution in Bahamian sediments. *Limnol. Oceanogr.* **47**, 1751–1763 (2002).
- Li, Y. et al. Soil carbon, nitrogen, and phosphorus stoichiometry and fractions in blue carbon ecosystems: implications for carbon accumulation in allochthonous-dominated habitats. *Environ. Sci. Technol.* **57**, 5913–5923 (2023).
- Short, F. T. Effects of sediment nutrients on seagrasses: literature review and mesocosm experiment. *Aquat. Bot.* **27**, 41–57 (1987).

36. Robbins, L. L., Tao, Y. & Evans, C. A. Temporal and spatial distribution of whittings on Great Bahama Bank and a new lime mud budget. *Geology* **25**, 947–950 (1997).
37. Perry, C. T. et al. Fish as major carbonate mud producers and missing components of the tropical carbonate factory. *Proc. Natl. Acad. Sci. USA* **108**, 3865–3869 (2011).
38. Enriquez, S. & Schubert, N. Direct contribution of the seagrass *Thalassia testudinum* to lime mud production. *Nat. Commun.* **5**, 3835 (2014).
39. Harris, P., Diaz, M. R. & Eberli, G. P. The formation and distribution of modern ooids on Great Bahama Bank. *Annu. Rev. Mar. Sci.* **11**, 491–516 (2019).
40. Ingalls, A. E., Aller, R. C., Lee, C. & Wakeham, S. G. Organic matter diagenesis in shallow water carbonate sediments. *Geochim. Cosmochim. Acta.* **68**, 4363–4379 (2004).
41. Burdige, D. J., Hu, X. & Zimmerman, R. C. The widespread occurrence of coupled carbonate dissolution/precipitation in surface sediments on the Bahamas Bank. *Am. J. Sci.* **310**, 492–521 (2010).
42. Koch, M. S. & Madden, C. J. Patterns of primary production and nutrient availability in a Bahamas lagoon with fringing mangroves. *Mar. Ecol. Prog. Ser.* **219**, 109–119 (2001).
43. Moran, K. L. & Bjorndal, K. A. Simulated green turtle grazing affects nutrient composition of the seagrass *Thalassia testudinum*. *Mar. Biol.* **150**, 1083–1092 (2007).
44. The Bahamas. First biennial update report to the United Nations Framework Convention on climate change. https://unfccc.int/sites/default/files/resource/2022_Dec_28%20-%20The%20Bahamas%20BUR1%20Submission%20to%20the%20UNFCCC%20-%20Approved.pdf (2022).
45. Duarte, C. M. & Krause-Jensen, D. Export from seagrass meadows contributes to marine carbon sequestration. *Front. Mar. Sci.* **4**, 13 (2017).
46. Shipley, O. N. et al. Energetic connectivity of diverse elasmobranch populations—implications for ecological resilience. *Proc. Royal Soc. B* **290**, 20230262 (2023).
47. Pathak, A., van Beynen, P. E., Akiwumi, F. A. & Lindeman, K. C. Impacts of climate change on the tourism sector of a Small Island Developing State: a case study for the Bahamas. *Environ. Dev.* **37**, 100556 (2021).
48. Kennedy, H. et al. Seagrass sediments as a global carbon sink: Isotopic constraints. *Global Biogeochem. Cycles* **24**, GB4026 (2010).
49. Johnson, R. A., Hanes, K. M., Bolten, A. B. & Bjorndal, K. A. Simulated green turtle grazing affects benthic infauna abundance and community composition but not diversity in a *Thalassia testudinum* seagrass meadow. *J. Exp. Mar. Biol. Ecol.* **522**, 151266 (2020).
50. Turschwell, M. P. et al. Anthropogenic pressures and life history predict trajectories of seagrass meadow extent at a global scale. *Proc. Natl. Acad. Sci. USA* **118**, e2110802118 (2021).
51. Serrano, O. et al. Impact of mooring activities on carbon stocks in seagrass meadows. *Sci. Rep.* **6**, 23193 (2016).
52. Brahim, M. B. et al. Variability in the structure of epiphytic assemblages of *Posidonia oceanica* in relation to human interferences in the Gulf of Gabes, Tunisia. *Mar. Environ. Res.* **70**, 411–421 (2010).
53. Diaz, M. R. et al. Geochemical evidence of microbial activity within ooids. *Sedimentology* **62**, 2090–2112 (2015).
54. Swart, P. K., Oehlert, A. M., Mackenzie, G. J., Eberli, G. P. & Reijmer, J. J. G. The fertilization of the Bahamas by Saharan dust: A trigger for carbonate precipitation? *Geology* **42**, 671–674 (2014).
55. Shinn, E. A. et al. African dust and the demise of Caribbean coral reefs. *Geophys. Res. Lett.* **27**, 3029–3032 (2000).
56. Food and Agriculture Organization of the United Nations (FAO). Global forest resources assessment 2005: Thematic study on mangrove, Bahamas. <https://www.fao.org/forestry/9179-045cf77fac860abf017c6833a248e7843.pdf>
57. Eyewitness News. Experts: 30% of Grand Bahama mangroves damaged by Dorian, 20% in Abaco (2022). <https://ewnews.com/experts-30-of-grand-bahama-mangroves-damaged-by-dorian-20-in-abaco> (2022).
58. Asplund, M. E. et al. Dynamics and fate of blue carbon in a mangrove–seagrass seascape: influence of landscape configuration and land-use change. *Landsc. Ecol.* **36**, 1489–1509 (2021).
59. Wabnitz, C. C., Andréfouët, S., Torres-Pulliza, D., Müller-Karger, F. E. & Kramer, P. A. Regional-scale seagrass habitat mapping in the Wider Caribbean region using Landsat sensors: Applications to conservation and ecology. *Remote Sens. Environ.* **112**, 3455–3467 (2008).
60. Abramoff, M. D., Magalhães, P. J. & Ram, S. J. Image processing with ImageJ. *Biophotonics Intern.* **11**, 36–42 (2004).
61. Howard, J., Hoyt, S., Isensee, K., Telszewski, M., & Pidgeon, E. Coastal blue carbon: methods for assessing carbon stocks and emissions factors in mangroves, tidal salt marshes, and seagrasses. (Conservation International, Intergovernmental Oceanographic Commission of UNESCO, International Union for Conservation of Nature, 2014).
62. Sanchez-Cabeza, J. A., Masqué, P. & Ani-Ragolta, I. ²¹⁰Pb and ²¹⁰Po analysis in sediments and soils by microwave acid digestion. *J. Radioanal. Nucl. Chem.* **227**, 19–22 (1998).
63. Krishnaswamy, S., Lal, D., Martin, J. M. & Meybeck, M. Geochronology of lake sediments. *Earth Planet. Sci. Lett.* **11**, 407–414 (1971).
64. Parnell, A. *simmr*: A Stable Isotope Mixing Model. R package version 0.4.5. Available at: <https://CRAN.R-project.org/package=simmr> (2021).
65. R Development Core Team. R: A language and environment for statistical computing. R Foundation for Statistical Computing. <http://www.R-project.org> (2023).
66. Fourqurean, J. W. & Schrlau, J. E. Changes in nutrient content and stable isotope ratios of C and N during decomposition of seagrasses and mangrove leaves along a nutrient availability gradient in Florida Bay, USA. *Chem. Ecol.* **19**, 373–390 (2003).
67. Kelleway, J. J., Trevathan-Tackett, S. M., Baldock, J. & Critchley, L. P. Plant litter composition and stable isotope signatures vary during decomposition in blue carbon ecosystems. *Biogeochemistry* **158**, 147–165 (2022).
68. Komada, T., Anderson, M. R. & Dorfmeier, C. L. Carbonate removal from coastal sediments for the determination of organic carbon and its isotopic signatures, $\delta^{13}\text{C}$ and $\Delta^{14}\text{C}$: comparison of fumigation and direct acidification by hydrochloric acid. *Limnol. Oceanogr. Methods* **6**, 254–262 (2008).
69. Fu, C. et al. Stocks and losses of soil organic carbon from Chinese vegetated coastal habitats. *Glob. Change Biol.* **27**, 202–214 (2021).
70. Bates, D., Mächler, M., Bolker, B. & Walker, S. Fitting Linear Mixed-Effects Models Using lme4. *J. Stat. Softw.* **67**, 1–48 (2015).

Acknowledgements

This research was funded by King Abdullah University of Science and Technology and Beneath The Waves with funding provided to C.M.D. (BAS/1/1071-01-01) and A.J.G. (Disney Conservation Fund, Pictet Foundation, Roger Sant and Doris Matsui, Code Blue Foundation, S. and K. Linblad, The Barry and Mimi Sternlicht Foundation, Pacific Treasure Foundation). We thank Beat Gasser and Inés Sanz Álvarez for laboratory work on the analysis of ²¹⁰Pb, Mongi Ennasri for help in C_{org} and isotope analysis, Kah Kheng Lim for assistance in statistical analysis. The IAEA is grateful for the support provided to its Marine Environment Laboratories by the Government of the Principality of Monaco.

Author contributions

C.M.D. designed this study. A.J.G. led and administered the overall research program in The Bahamas. S.F., M.N.H., W.H., S.D.H., E.L., A.J.G., and C.M.D. conducted the fieldwork. C.F., W.H., and P.M. conducted the laboratory measurements. C.F. and C.M.D. wrote the original manuscript. All authors contributed to reviewing and editing of the manuscript.

Competing interests

The authors declare no competing interests.

Additional information

Supplementary information The online version contains supplementary material available at <https://doi.org/10.1038/s43247-023-01154-0>.

Correspondence and requests for materials should be addressed to Chuancheng Fu.

Peer review information *Communications Earth & Environment* thanks Samantha Garrard, Maria Emilia Rohr, and Manon Picard for their contribution to the peer review of this work. Primary handling editors: José Luis Iriarte Machuca and Clare Davis. A peer review file is available.

Reprints and permission information is available at <http://www.nature.com/reprints>

Publisher's note Springer Nature remains neutral with regard to jurisdictional claims in published maps and institutional affiliations.



Open Access This article is licensed under a Creative Commons Attribution 4.0 International License, which permits use, sharing, adaptation, distribution and reproduction in any medium or format, as long as you give appropriate credit to the original author(s) and the source, provide a link to the Creative Commons licence, and indicate if changes were made. The images or other third party material in this article are included in the article's Creative Commons licence, unless indicated otherwise in a credit line to the material. If material is not included in the article's Creative Commons licence and your intended use is not permitted by statutory regulation or exceeds the permitted use, you will need to obtain permission directly from the copyright holder. To view a copy of this licence, visit <http://creativecommons.org/licenses/by/4.0/>.

© The Author(s) 2023